


An assessment of commonly employed satellite-based remote sensors for mapping mangrove species in Mexico using an NDVI-based classification scheme

L. Valderrama-Landeros · F. Flores-de-Santiago  ·
J. M. Kovacs · F. Flores-Verdugo

Received: 17 August 2017 / Accepted: 5 December 2017 / Published online: 14 December 2017
© Springer International Publishing AG, part of Springer Nature 2017

Abstract Optimizing the classification accuracy of a mangrove forest is of utmost importance for conservation practitioners. Mangrove forest mapping using satellite-based remote sensing techniques is by far the most common method of classification currently used given the logistical difficulties of field endeavors in these forested wetlands. However, there is now an abundance of options from which to choose in regards to satellite sensors, which has led to substantially different estimations of mangrove forest location and extent with particular concern for degraded systems. The objective of this study was to assess the accuracy of mangrove forest classification using different remotely sensed data sources (i.e., Landsat-8, SPOT-5, Sentinel-2, and

WorldView-2) for a system located along the Pacific coast of Mexico. Specifically, we examined a stressed semiarid mangrove forest which offers a variety of conditions such as dead areas, degraded stands, healthy mangroves, and very dense mangrove island formations. The results indicated that Landsat-8 (30 m per pixel) had the lowest overall accuracy at 64% and that WorldView-2 (1.6 m per pixel) had the highest at 93%. Moreover, the SPOT-5 and the Sentinel-2 classifications (10 m per pixel) were very similar having accuracies of 75 and 78%, respectively. In comparison to WorldView-2, the other sensors overestimated the extent of *Laguncularia racemosa* and underestimated the extent of *Rhizophora mangle*. When considering such type of sensors, the higher spatial resolution can be particularly important in mapping small mangrove islands that often occur in degraded mangrove systems.

L. Valderrama-Landeros
Subcoordinación de Percepción Remota, Comisión Nacional Para el Conocimiento y Uso de la Biodiversidad (CONABIO), 4903 Liga Periférico-Insurgentes Sur, 14010 Tlalpan, CDMX, Mexico

F. Flores-de-Santiago (✉)
Instituto de Ciencias del Mar y Limnología, Unidad Académica Procesos Oceánicos y Costeros, Universidad Nacional Autónoma de México, A.P. 70-305, Av. Universidad 3000, Ciudad Universitaria, 04510 Coyoacán, CDMX, Mexico
e-mail: floresdesantiago@gmail.com
e-mail: ffloresd@cmar.unam.mx

J. M. Kovacs
Department of Geography, Nipissing University, 100 College Dr, North Bay, ON P1B 8L7, Canada

F. Flores-Verdugo
Instituto de Ciencias del Mar y Limnología, Unidad Académica Mazatlán, Universidad Nacional Autónoma de México, Av. Joel Montes Camarena s/n, 82040 Mazatlán, SIN, Mexico

Keywords Landsat-8 · SPOT-5 · Sentinel-2 · WorldView-2 · Forested wetland

Introduction

Mangrove forests are located at the intertidal zone of estuaries, coastal lagoons, and open shorelines along tropical and subtropical coastlines (Saintilan et al. 2014). These ecosystems are of utmost importance for local communities providing fishery products (e.g., fish, shrimp, crabs, mollusks), timber goods (e.g., firewood, construction materials), and recreational uses such as eco-tourism (Walters et al. 2008; Mukherjee et al.

2014). They also support a number of key ecosystem services such as habitat for aquatic (Martin et al. 2015) and non-aquatic faunal species (Ferreira et al. 2015), coastal protection (Horstman et al. 2015), carbon sequestration and storage (Alongi 2016), and treatment of brackish water from aquaculture (De-León-Herrera et al. 2015). However, mangroves undergo threats from direct impacts such as coastal development projects (e.g., aquaculture, tourist industry) and pollution (Duke 2016), as well as from indirect impacts such as changes in inland freshwater management and various forms of hydrological modifications (e.g., roads, channels), which are threatening their health and resilience. Of key concern is the first appearance of a great-scale mangrove die back which is most likely attributed to climate change (Duke et al. 2017). Indeed, current mangrove forest destruction and degradation is equal to or greater than that of other more appealing ecosystems losses, such as coral reefs and rainforest (Duke et al. 2007), and not surprising, focus of great concern by the United Nations Environment Programme (van Bochove et al. 2014).

Given the ecological and economical importance of mangrove forests, there is an increasing need to monitor and evaluate their condition and geographical distribution in order to help guide conservation and restoration efforts (Dronova 2015). Since many mangrove forests are difficult to access, due to the flooded, soft sediment environments in which they grow, the ability to accurately estimate large areas of mangrove cover and rates of change with remote sensing data would greatly assist in these endeavors (Fries and Webb 2014). Remote sensing platforms have the advantages of being large-scale, long-term, and in some cases cost-effective monitoring approaches (Kuenzer et al. 2011). Consequently, mapping of mangrove forests using remote sensing techniques has been widely used and is frequently a reliable alternative to extensive ground-survey methods of mapping, mainly in remote or inaccessible regions (Guo et al. 2017). For instance, in mangrove forest management, remote sensing applications could provide key information regarding habitat inventories at species level (e.g., Kovacs et al. 2005; Kovacs et al. 2010), pigment content assessments (e.g., Heenkenda et al. 2015; Flores-de-Santiago et al. 2016), change detection and monitoring (e.g., Ibharim et al. 2015; Son et al. 2016), distribution along latitudinal limits (e.g., Otero et al. 2016; Ximenes et al. 2016), and overall ecosystem evaluation (e.g., McCarthy et al. 2015).

Fast and accurate mapping is the key component for sustainable conservation of mangrove forests (Chadwick 2011). It is clear that conventional remote sensing images are now used for operational mapping and monitoring of mangroves (Pettorelli et al. 2014). However, the spatial and spectral information provided by these conventional data may not be enough for studying mangrove forests and their species composition in detail (Ximenes et al. 2016; McCarthy et al. 2015). For example, broad separation of mangrove forests from surrounding tropical rain forests or other more arid ecosystems is feasible with traditional sensors and digital elevation models (Alsaaidh et al. 2013), but studies using remote sensing techniques to assess in more detail the diversity within mangrove species are still uncommon (e.g., Flores-de-Santiago et al. 2013a; Heenkenda et al. 2014; Zhang et al. 2014). For instance, Friess and Webb (2014) demonstrated that high variance in mangrove estimates leads to highly variable deforestation trends, depending on the original data source and the criteria used for classification. Moreover, detailed mangrove forest characterization is difficult with moderate spatial resolution (~30 m) satellite data due to the often-narrow extent along coastlines, which sometimes delivers contradictory results (see assessment by Kovacs et al. 2009). Consequently, in order to describe these ecosystems more accurately in terms of their physiognomic classification and diversity patterns, the combination of higher spatial (4 m or less) and spectral resolutions are thus suggested (Wang et al. 2016).

Vegetation indices (VI) are widely used as key indicators for assessing the environmental variations of land cover among vegetative targets. The Normalized Difference Vegetation Index (NDVI) is one of the more popular methods in vegetation monitoring (Pettorelli 2013), including mangrove forests. For instance, Kovacs et al. (2004, 2005, 2009) used NDVI to estimate Leaf Area Index (LAI) and considered very-high spatial resolution data a useful tool for mangrove species discrimination analysis in order to minimize logistical and practical difficulties of field work in inaccessible mangrove areas. Nevertheless, it must be pointed out that the NDVI is not always identified as the optimal VI for mangrove leaf chlorophyll estimates (Flores-de-Santiago et al. 2013b; Flores-de-Santiago et al. 2016). Clearly, higher spatial resolution improves the results at which mangroves are mapped using satellite imagery (Lee and Yeh 2009). It is for this reason that

conventional, often freely available, satellite images have not been extensively used for mapping mangrove at the species level. Moreover, given the small patch size of some degraded mangrove forests stands, typical of many semiarid regions, it has been suggested that spatial resolution plays a more important role in discriminating different mangrove species (Friess and Webb 2014).

Although the higher spatial resolution data are recommended, there are many concerns in their use including increase data volume and the higher cost of data acquisition, storage, and processing. As such, it is desirable to use an optimal spatial resolution for a given study that will be affected by the spatial composition and structure of the scene, and by the information of the target to be extracted. In this sense, optimal spatial resolution is the one at which the information content per pixel is maximized (Jensen 2016) and it will depend on the mangrove species, the forest age, and the spectral bands used. It is apparent that distinguishing the canopies of different mangrove species with conventional medium sensors such as Landsat and SPOT is a difficult if not impossible endeavor due to the coarse spectral and spatial resolution of such images (Friess and Webb 2014). For example, such sensors could be unsuitable for separating the relatively small clusters (i.e., islands) typical of degraded mangrove stands, which in some situations exhibit very similar spectral signatures (Flores-de-Santiago et al. 2016).

The recent advancement of very-high spatial resolution, multispectral satellite sensors makes it possible to remotely assess mangrove species at a spatial resolution below a meter (Kuenzer et al. 2011). Hence, an improved classification of individual mangrove species is now possible. However, with this enhancement comes the task of developing more complex analytical approaches such as object-based image analysis (e.g., Flores-de-Santiago et al. 2013a) that can realize the full potential of the acquired data when attempting to separate mangrove classes. Nevertheless, it is clear that the development of new methods for mapping mangrove forests by collecting information with very-high spatial resolution sensors and VIs, particularly at the species and physiognomic levels, is still at an early assessment stage. Hence, the purpose of this investigation was to assess the utility of several satellite sensors with various spatial resolutions (i.e., Landsat-8, SPOT-5, Sentinel-2, and WorldView-2) for mapping mangrove species and conditions along a degraded mangrove forests of the

Mexican Pacific. Results from this investigation could provide reliable information for future national inventories particularly those with similar species and conditions.

Materials and methods

Study area

The Teacapán-Agua Brava-Las Haciendas estuarine system is located along the Pacific coast of Mexico on the border between the states of Sinaloa and Nayarit (Fig. 1). This system is considered the largest mangrove habitat on the Pacific coast of the Americas, with an estimated overall extension of 80,000 ha of mangroves and 150,000 ha of seasonal floodplains (Blanco-Correa 2011). The Agua Brava Lagoon, which is located in the south, supports an extensive mangrove community where the red mangrove (*Rhizophora mangle*) is present along the edge of the many tidal channels, and the white mangrove (*Laguncularia racemosa*) is commonly found where the tidal influence is minimal. There are two channels that connect the system with the Pacific Ocean, a natural inlet in Teacapán and an artificial inlet known as the Cautla Canal. Unfortunately, the mangrove forests have experienced considerable degradation since the opening of the Cautla Canal in 1973, which was reported by local fishermen (Kovacs 2000) and first mapped using Landsat data (Kovacs et al. 2001). Moreover, it is believed that the hypersaline conditions, commonly found in the north section of the study area, caused the mangroves to fragment into small, very-dense clusters, which was confirmed by the recent oblique photos taken from a helicopter and from field campaigns (Fig. 2).

Regarding mapping endeavors in the area, Blanco-Correa (2011) did a comprehensive analysis about the change in land use including hydrological and geomorphological assessments; more recently, Troche-Souza et al. (2016) mapped the entire mangrove system based on SPOT-5 data. Additional detailed analysis has been performed in specific areas. For instance, Kovacs et al. (2005) conducted the first study that used very-high spatial resolution IKONOS data and in situ LAI-2000 sensor data in order to create a map of mangroves at the species level. Moreover, Kovacs et al. (2009) pointed out the need of field validation and optimal spatial resolution data for mangrove assessments.

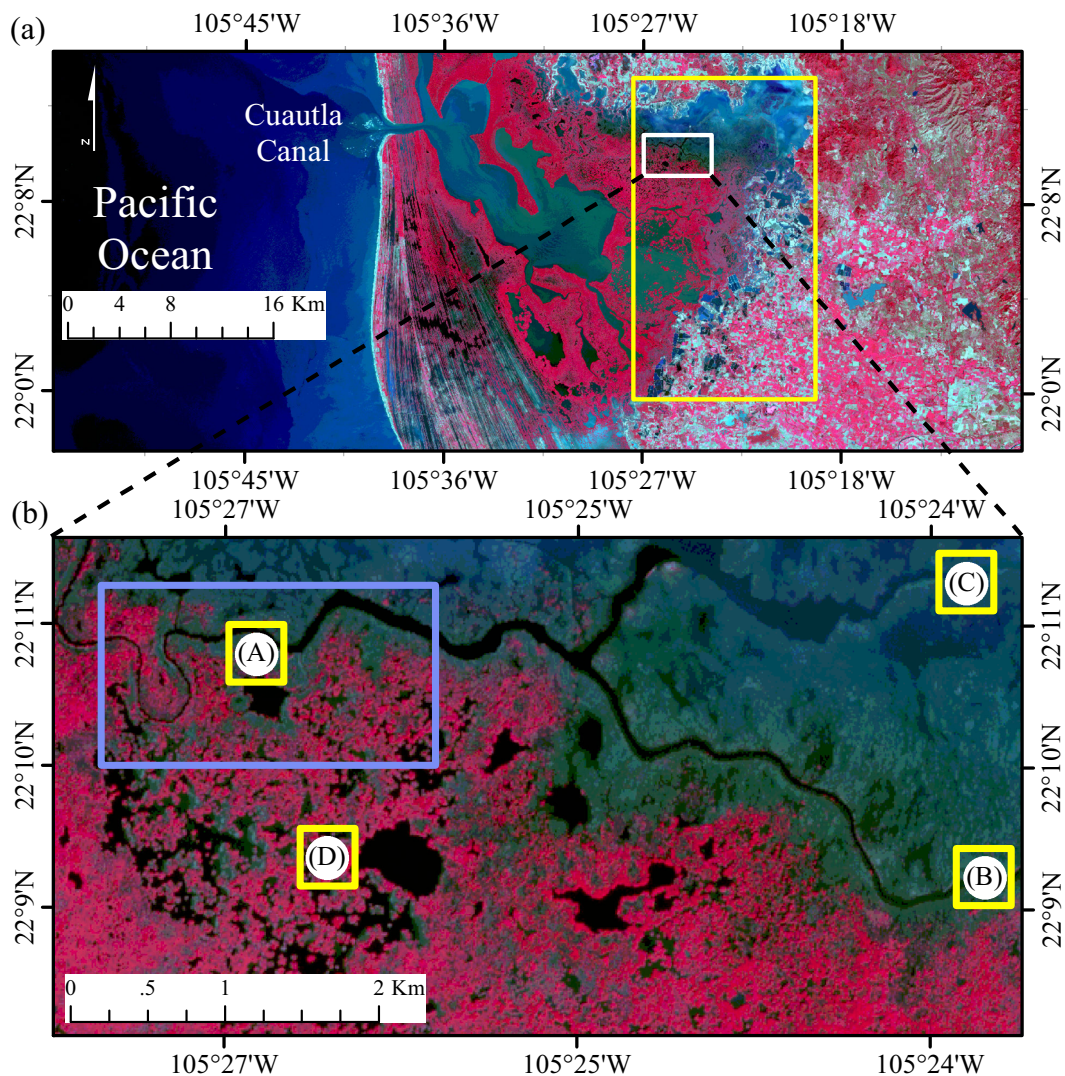


Fig. 1 **a** Location of the mangrove forest study area at the north-easter section of the Agua Brava coastal lagoon, Pacific coast of Mexico (Enhanced Near infrared, Red, Green of Sentinel-2 dated January 12, 2016). The yellow rectangle represents the boundary

for the classification process. **b** Degraded area test site with four representative locations (A), (B), (C), and (D). The purple rectangle denotes an example of the oblique photos taken from the helicopter depicted in Fig. 2

Satellite data processing and field survey

A variety of commonly available satellite data were acquired for the study area (Table 1). Radiometric and atmospheric corrections were performed using the software PCI-Geomatica 2015 and QGIS. Specifically, the ATCOR model (Richter and Schläpfer 2016) was performed on the WorldView-2 data, the Geosud Toa Reflectance (Ose 2015) on the Landsat-8 and SPOT-5, and the Semi-Automatic Classification Plugin (Congedo 2016) on the Sentinel-2 data. In order to geometrically correct the images, 34 ground control points (GCP) were

employed using a UTM zone 13 map projection, then a mask was created of open water using the near-infrared band (NIR) for each image (Table 1). A second mask was manually created in order to separate agricultural fields, aquaculture ponds, and saltpan located at the eastern part of the study site. Specifically, in this area, it is quite feasible to discriminate mangrove forests from the aforementioned land-cover types by visual inspection.

Following a previous mangrove forest investigation at the species level for this study area (Kovacs et al. 2005), we selected three mangrove classes: (1) dominant red mangrove (*Rhizophora mangle*) stands, (2) dominant

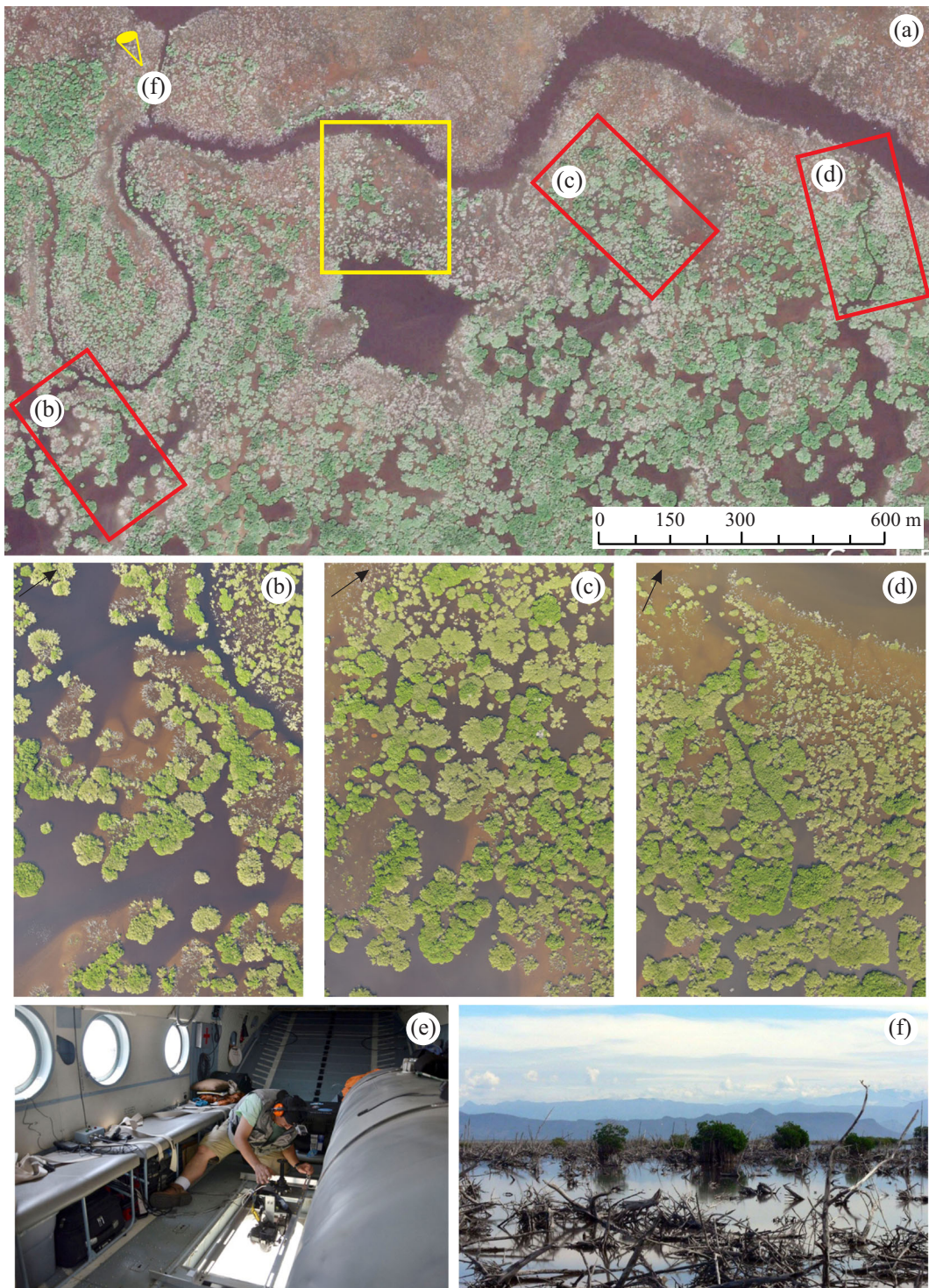


Fig. 2 a Examples of mangrove degraded islands at the north section of the study area. The yellow rectangle represents location of site (A) from Fig. 1. b, c, d Oblique photos taken from a

helicopter (e) (SEMAR-CONABIO 2016). f Location of a field photo of the degraded mangrove site

Table 1 Optical data specifications collected for the study area

Sensor	Date of acquisition (month/day/year)	Time of acquisition (GMT)	Pixel spacing (m)	Red band (nm)	Near-infrared band (nm)
Landsat-8	5/29/2015	17:29:11	30	640–670	850–880
SPOT-5	11/26/2014	16:48:37	10	610–680	780–890
Sentinel-2	1/12/2016	17:49:16	10	650–680	785–900
WorldView-2	4/4/2015	17:47:29	1.6	630–690	760–900

white mangrove (*Laguncularia racemosa*) stands, and (3) dead mangrove stands. Based on the number of selected classes and according to Lillesand et al. (2008), a total of 120 circular sample stations, 40 per class, were selected within the study area. Each station was designated based on a previous fieldwork campaign, and for each station; a radius of 6.9 m from the center was recorded covering an area of 0.015 ha using the software QGIS 2.18. For each station, an NDVI value was then calculated from each of the satellite data sources for all pixels except for those considered open water. Specifically, we used the (NIR) wavelengths for each data (Table 1).

Data extraction and accuracy assessment

For each image, we extracted the NDVI intervals of all mangrove classes within the 120 stations. Specifically, the mean, median, minimum, and maximum values were recorded and compared using boxplots. The level of classification was performed with the three mangrove classes (*Rhizophora mangle*, *Laguncularia racemosa*, dead mangrove) and open water. Based on the NDVI intervals per class, decision trees classifications were developed for all satellite data. For the accuracy assessment, we calculated the optimum sample size for the error matrix based on the following equation by Congalton and Green (1999), using the multinomial distribution approach shown in Eq. (1):

$$N = (Z^2 pq / E^2), \quad (1)$$

where N is the optimum number of sample points, p is the percentage calculated accuracy, q is the $100-p$, E is the allowed error, and Z is the standard normal deviate for the confidence level.

The resulting minimum random point number was 204. The accuracy was assessed using the error matrices and their associated statistics: overall accuracy, class producer's accuracy, class user's accuracy, and the kappa statistics (Jensen 2016). To test the accuracy for each

image, the same 204 ground truth validation points were maintained. All points were verified using the previous classification map of Kovacs et al. (2005), oblique photos taken from a helicopter, and field knowledge of the study site (Fig. 2). The producer's and user's accuracies were examined for individual class assessments when the overall accuracy was deemed similar among images. Additionally, the total area (ha) and percentage of each class were calculated for each classification.

Results

The box plots derived from the NDVI intervals among the four-satellite data show that the dead mangrove class is clearly separated from the live trees (Fig. 3). Overall,

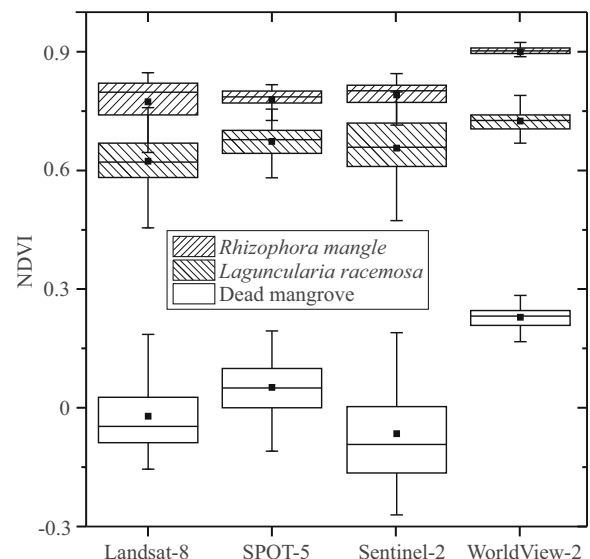


Fig. 3 Normalized Difference Vegetation Index (NDVI) box plots for three classes (*Rhizophora mangle*, *Laguncularia racemosa*, and dead mangrove). Each box plot depicts the mean (small square), the 25–75% quartiles (rectangle), and the median (line dividing the box plot) extracted from the five remote sensing images: Landsat-8, SPOT-5, Sentinel-2, and WorldView-2

the *Rhizophora mangle* NDVI intervals were higher compared to that of *Laguncularia racemosa* values for all sensors. However, the WorldView-2 data was the only satellite sensor in which *Laguncularia racemosa* and *Rhizophora mangle* could be utterly separated from each other. The remaining three satellite data presented some degree of NDVI mixture between both live mangrove classes, principally between the upper limit of the *Laguncularia racemosa* with the lower limit of the *Rhizophora mangle* values. Particularly, Sentinel-2 data was the sensor that showed more mixed NDVI values between mangrove species.

The overall mangrove classification results from the four satellite data indicated that the dead mangrove zone was located at the northeastern section of the study area, while the *Rhizophora mangle* was found close to the main tidal channels and the *Laguncularia racemosa* stands in the less frequent tidal flushing zones (Fig. 4). Regarding the accuracy assessment, Landsat-8 (30 m)

gave a minimal and overall accuracy of 64% (Table 2), SPOT-5 (10 m) of 75% (Table 3), Sentinel-2 (10 m) of 78% (Table 4), and WorldView-2 (1.6 m) of 93% (Table 5). With the exception of the WorldView-2 data, there were many issues related to misclassification in areas classified as open water typically located in the central part of the study area. However, the NDVI intervals between *Rhizophora mangle* and *Laguncularia racemosa* were well discriminated in the box plots for the WorldView-2 data with user’s accuracies for both mangrove classes at 94% and 90%, respectively. Moreover, the overall and user’s accuracies of the Sentinel-2 classification performed better compared to the Landsat-8 and SPOT-5 classifications.

The total open water area and dead mangrove stands did not vary among the four remote sensors covering 63% and 8% respectively (Table 6). The most problematic classification mapping issue was the discrimination of *Rhizophora mangle* from

Fig. 4 Classified map of mangrove forests derived from the intervals of NDVI values for the study site. Landsat-8 (a), SPOT-5 (b), Sentinel-2 (c), and WorldView-2 (d)

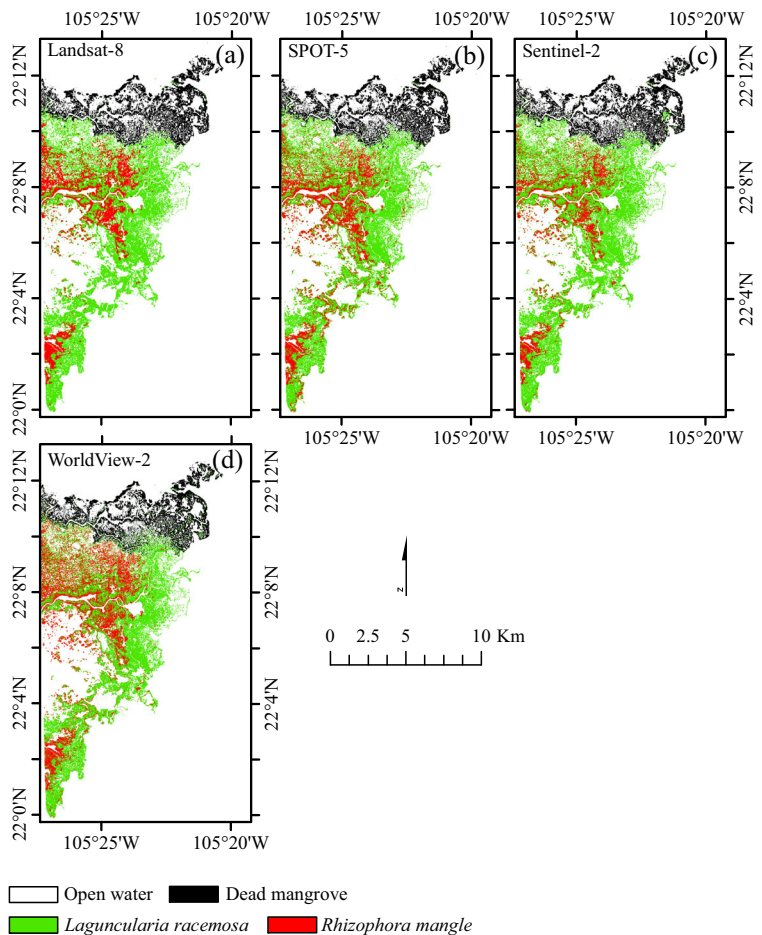


Table 2 The error matrix for the Landsat-8 data classification

Class	Reference data				User's accuracy (%)
	Open water	Dead mangrove	<i>Laguncularia racemosa</i>	<i>Rhizophora mangle</i>	
Open water	0	6	21	8	0
Dead mangrove	0	28	5	0	85
<i>Laguncularia racemosa</i>	0	3	73	21	75
<i>Rhizophora mangle</i>	0	0	9	30	77
Producer's accuracy (%)	ND	76	68	51	
Overall accuracy (%)	64				
Overall kappa statistics	0.46				

Laguncularia racemosa stands. For instance, if we take into consideration the WorldView-2 image as the best classification, all sensors overestimated, to some extent, *Laguncularia racemosa* and underestimated *Rhizophora mangle* hectares (Table 6). It is clear from the classification maps (Fig. 4) that the major underestimation of *Rhizophora mangle* occurred in the northeastern section of the study area where many mangrove clusters are found. Nevertheless, Sentinel-2 presented higher user's accuracies for both mangrove classes and Landsat-8 the lowest user's accuracies (Tables 2 and 4).

Figure 5 depicts four representative locations in this study area: (a) degraded mangrove islands with *Rhizophora mangle* and *Laguncularia racemosa* stands; (b) fringe *Laguncularia racemosa*; (c) dead mangrove; and (d) healthy mangrove islands with *Rhizophora mangle* and *Laguncularia racemosa* stands. All but the WorldView-2 misclassified *Laguncularia racemosa* in many sections along the main tidal channels of the degraded stands (Fig. 2 a, b, c), and for small islands

covered by *Rhizophora mangle* (Fig. 5 d). Hence, the spatial resolution of the sensors played a key role in fragmented mangrove stands.

Discussion

Results from this investigation provide quantitative evidence that the spatial resolution is of utmost importance in mapping of mangrove forests using the same classification approach for this region of Mexico. This study shows that very-high spatial resolution multispectral imagery from WorldView-2 data can effectively map the spatial distribution of mangrove species at regional scales. Contrary, very small and dense clusters (i.e., islands) of mangrove forests along the tidal creeks will not be identified from moderate-resolution satellite data such as Landsat-8, SPOT-5, and Sentinel-2.

Currently, the great contradictions in trends of mangrove forests extent suggests that estimates of

Table 3 The error matrix for the SPOT-5 data classification

Class	Reference data				User's accuracy (%)
	Open water	Dead mangrove	<i>Laguncularia racemosa</i>	<i>Rhizophora mangle</i>	
Open water	0	2	8	3	0
Dead mangrove	0	32	3	2	86
<i>Laguncularia racemosa</i>	0	3	86	18	80
<i>Rhizophora mangle</i>	0	0	11	36	77
Producer's accuracy (%)	ND	86	79	61	
Overall accuracy (%)	75				
Overall kappa statistics	0.61				

Table 4 The error matrix for the Sentinel-2 data classification

Class	Reference data				User’s accuracy (%)
	Open water	Dead mangrove	<i>Laguncularia racemosa</i>	<i>Rhizophora mangle</i>	
Open water	0	3	8	6	0
Dead mangrove	0	33	3	0	92
<i>Laguncularia racemosa</i>	0	1	93	19	82
<i>Rhizophora mangle</i>	0	0	4	34	89
Producer’s accuracy (%)	ND	89	86	58	
Overall accuracy (%)	78				
Overall kappa statistics	0.65				

ecosystem health, mangrove loss, biodiversity threat assessments, and conservation policies will be hampered by low confidence in mangrove classification (Friess and Webb 2014). In fact, isolated clusters of mangrove stands from arid/semiarid regions influences mapping accuracies (Gao 1998). In these climatically stressful zones, mangroves do not grow as extensively as those in tropical latitudes (Flores-Verdugo et al. 1987). In general, each cluster of mangrove forest is small-sized and elongated in shape due to hypersaline conditions. Although these clusters could extent over a large area, as seen in Fig. 3, each patch registers merely a couple of pixels in the Landsat-8, SPOT-5, and Sentinel-2 images. During the classification accuracy, the isolated clusters of mangroves of a few pixels are generalized and replaced by other classes causing misclassification with, for example, water bodies (Fig. 4) resulting in lower user’s accuracies for the Landsat-8, SPOT-5, and Sentinel-2 data. Our field work campaign confirmed that most of this mangrove system at the test site is under severe degradation, and the mangrove trees

are often on small islands with narrow tidal channels (approximately 10–30 m wide strips). Hence, the 30 m × 30 m pixels of Landsat-8 did not resolve these areas or the mixed mangrove vegetation that were aggregated within each 30 m pixel. Contrary, the SPOT-5 and Sentinel-2 were able to separate at some degree both species, but similar difficulties compared to the Landsat-8 were found. As expected, the very-high spatial resolution of the WorldView-2 data help discriminate these mangrove classes extremely well. In theory, the results between the SPOT-5 and the Sentinel-2 classifications should be similar due to their identical spatial resolution. However, the overall accuracy was higher in the Sentinel-2 data as well as the user’s accuracies for both mangrove species. This could be a consequence of the higher radiometric resolution of the Sentinel-2 (12 bit) in comparison to the SPOT-5 (8 bit).

Utilizing remote sensing assessments allow us to determine the specific sites of the most vulnerable mangrove locations (Vo et al. 2015). Such knowledge plays a key role in the decision-making process for future

Table 5 The error matrix for the WorldView-2 data classification

Class	Reference data				User’s accuracy (%)
	Open water	Dead mangrove	<i>Laguncularia racemosa</i>	<i>Rhizophora mangle</i>	
Open water	0	0	0	0	100
Dead mangrove	0	36	0	0	100
<i>Laguncularia racemosa</i>	0	1	105	11	90
<i>Rhizophora mangle</i>	0	0	3	48	94
Producer’s accuracy (%)	ND	97	97	81	
Overall accuracy (%)	93				
Overall kappa statistics	0.88				

Table 6 Land cover classification (ha) and percentage (%) of the four remote sensing platforms

Class	Sensor			
	Landsat-8	SPOT-5	Sentinel-2	WorldView-2
Open water	13,778 (63%)	13,767 (63%)	13,763 (63%)	13,765 (63%)
Dead mangrove	1780 (8%)	1767 (8%)	1802 (8%)	1675 (8%)
<i>Laguncularia racemosa</i>	4861 (22%)	4652 (21%)	5106 (23%)	4514 (21%)
<i>Rhizophora mangle</i>	1548 (7%)	1781 (8%)	1296 (6%)	2013 (8%)
Total area	21,969	21,967	21,967	21,967

restoration efforts. It has been suggested that moderate resolution satellite data such as Landsat contain enough detail to capture mangrove forest distribution and

dynamics (Giri et al. 2011). In the present study, the total mangrove extent area did not vary considerably among the coarse spatial resolution images (Table 6).

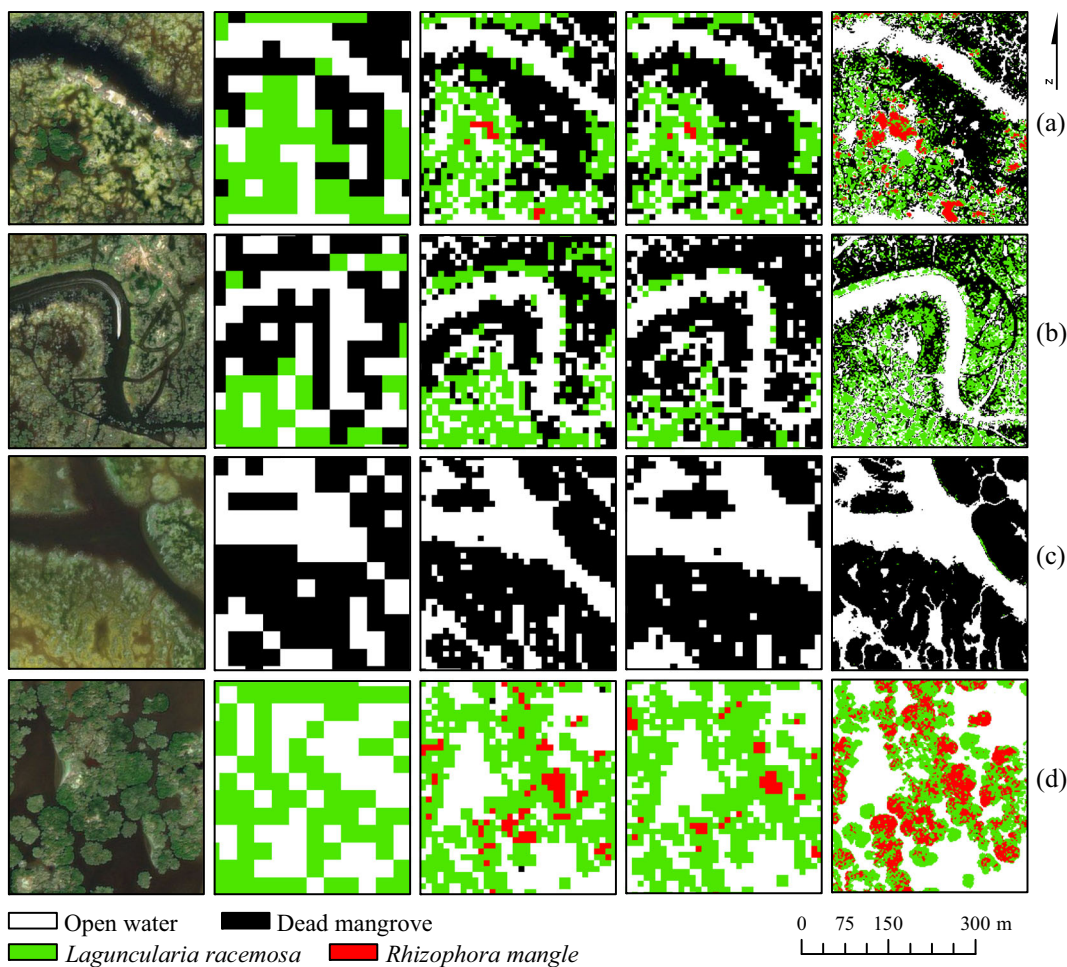


Fig. 5 Examples of representative locations from the mangrove classifications using an NDVI approach. From left to right: True color WorldView-2 image; Landsat-8 classification; SPOT-5 classification; Sentinel-2 classification; and WorldView-2 classification. **a** Degraded mangrove islands with *Rhizophora mangle* and

Laguncularia racemosa stands; **b** fringe *Laguncularia racemosa* zone; **c** dead mangrove area; and **d** healthy mangrove islands with *Rhizophora mangle* and *Laguncularia racemosa* stands. The scale is 1:10,000

However, the spatial resolution of Landsat-8, SPOT-5, and Sentinel-2 hinders the mapping of specific locations of mangrove species within the study site (Fig. 5). Clearly, very high-resolution images or oblique aerial photographs are needed to assess and monitor those very small clusters (Green et al. 1998). However, there are only a few cases where mangrove species have been classified at this level of detail within an individual system due to the higher cost of very-high spatial resolution data (Kovacs et al. 2005).

This study shows that very high-resolution multi-spectral data can effectively map the spatial distribution of mangroves at regional scales in a degraded area. However, it is important to recognize the limitations of this work. For instance, the use of the single NDVI method may produce serious errors in biomass estimation (Li et al. 2007). Also, the NDVI is not always identified as the optimal estimator of chlorophyll-a content in subtropical mangroves (Flores-de-Santiago et al. 2013b) as well as chlorophyll-b and total carotenoids (Flores-de-Santiago et al. 2016). The NDVI only reflects the crown information of mangrove trees, and thus the vertical profile (e.g., tree height) cannot be retrieved by this VI (Li et al. 2007). Additionally, the study site presents two physiognomic communities of *Laguncularia racemosa* that includes a relatively healthy forest closer to the tidal channels and a more degraded one located more inland (Kovacs et al. 2005). Thereby, not all images will be suitable for a more detailed classification of the various physiognomic states of *Laguncularia racemosa* stands. Moreover, WorldView-2 data could be crucial in determining pigment content given the Red-edge band which could improve mangrove discrimination (Flores-de-Santiago et al. 2016). Indeed, Koedsin and Vaiphasa (2013) classified five mangrove species with high-spectral resolution Hyperion data (30 m per pixel) in Thailand achieving an overall accuracy of 92%. It is clear that future studies should assess mangrove forest inventories using different classification methods and different spectral bands whenever possible.

Conclusions

Optimal spatial resolution from remote sensing data is needed to classify and monitor environmental variability in mangrove forests, which are currently threatened by coastal development, aquaculture expansion, freshwater

diversion, and climate change. Mangrove species were difficult to discriminate in multispectral imagery with coarse spatial resolution because of similarities in their spectral reflectance properties. However, the failure of the NDVI in coarse spatial resolution data does not necessarily preclude their applicability in other more tropical latitudes where mangrove forests thrive under optimal conditions. Given the spatial dynamics of highly dense small clusters of mangrove species, it is clear that the type of remote sensing data used during the classification procedure can substantially affect the accuracy of the final mangrove map. Comparing mangrove species mapping using a standard method of classification among different remote sensing platforms is a key step in determining the optimal spatial resolution for monitoring purposes. We believe that the present study is the first to include a single method of classification among different spatial resolution images for a degraded mangrove forest. The accuracy issues presented in our results could be of utmost importance for future studies regarding mangrove forests inventories at the national level in countries where acquisition of very-high spatial resolution data is limited.

Acknowledgements LVL acknowledge financial support for the WorldView-2 data acquisition and field work campaigns in 2015 through the Packard Foundation and the Fondo Mexicano para la Conservación de la Naturaleza (FMCN). FFS appreciate the financial support through a grant provided by the Dirección General de Asuntos del Personal Académico, Universidad Nacional Autónoma de México (DGAPA-UNAM, Mexico). We thank the Mexican Navy (SEMAR) for the helicopter flights and oblique photos collection.

References

- Alongi, D. M. (2016). Mangroves. In M. J. Kennish (Ed.), *Encyclopedia of estuaries* (pp. 393–404). New York: Springer. https://doi.org/10.1007/978-94-017-8801-4_3.
- Alsaadeh, B., Al-Hanbali, A., Tateishi, R., Kobayashi, T., & Hoan, N. T. (2013). Mangrove forests mapping in the southern part of Japan using Landsat ETM+ with DEM. *Journal of Geographic Information Systems*, 5(04), 369–377. <https://doi.org/10.4236/jgis.2013.54035>.
- Blanco-Correa, M. (2011). *Diagnóstico funcional de Marismas Nacionales*. Tepic: Informe final de los convenios de coordinación entre la Universidad Autónoma de Nayarit y la Comisión Nacional Forestal con el patrocinio del Gobierno del Reino Unido.
- Chadwick, J. (2011). Integrated LiDAR and IKONOS multispectral imagery for mapping mangrove distribution and physical

- properties. *International Journal of Remote Sensing*, 32(21), 6765–6781. <https://doi.org/10.1080/01431161.2010.512944>.
- Congalton, R., & Green, K. (1999). *Assessing the accuracy of remotely sensed data: principles and practices*. Boca Raton: CRC/LEWIS Press.
- Congedo, L. (2016). Semi-automatic classification plugin documentation. Technical report. <https://doi.org/10.13140/RG.2.2.29474.02242/1>. Accessed 14 Nov 2017.
- De-León-Herrera, R., Flores-Verdugo, F., Flores-de-Santiago, F., & González-Farías, F. (2015). Nutrient removal in a closed silvofishery system using three mangrove species (*Avicennia germinans*, *Laguncularia racemosa*, and *Rhizophora mangle*). *Marine Pollution Bulletin*, 91(1), 243–248. <https://doi.org/10.1016/j.marpolbul.2014.11.040>.
- Dronova, I. (2015). Object-based image analysis in wetland research: A review. *Remote Sensing*, 7(5), 6380–6413. <https://doi.org/10.3390/rs70506380>.
- Duke, N. C. (2016). Oil spill impacts on mangroves: recommendations for operational planning and action based on a global review. *Marine Pollution Bulletin*, 109(2), 700–715. <https://doi.org/10.1016/j.marpolbul.2016.06.082>.
- Duke, N. C., Meynecke, J. O., Dittmann, S., Ellison, A. M., Anger, K., Berger, U., Cannicci, S., Diele, K., Ewel, K. C., Field, C. D., Koedam, N., Lee, S. Y., Marchand, C., Nordhaus, I., & Dahdouh-Guebas, F. (2007). A world without mangroves? *Science*, 317(5834), 41–42. <https://doi.org/10.1126/science.317.5834.41b>.
- Duke, N. C., Kovacs, J. M., Griffiths, A. D., Preece, L., Hill, D. J. E., van Oosterzee, P., Mackenzie, J., Morning, H. S., & Burrows, D. (2017). Large-scale dieback of mangroves in Australia's Gulf of Carpentaria: a severe ecosystem response, coincidental with an unusually extreme weather event. *Marine and Freshwater Research*, 68(10), 1816–1829. <https://doi.org/10.1071/MF16322>.
- Ferreira, A. C., Ganade, G., & Attayde, J. L. D. (2015). Restoration vs natural regeneration in neotropical mangrove: effects on plant biomass and crab communities. *Ocean and Coastal Management*, 110, 38–45. <https://doi.org/10.1016/j.ocecoaman.2015.03.006>.
- Flores-de-Santiago, F., Kovacs, J. M., & Lafrance, P. (2013a). An object-oriented classification method for mapping mangroves in Guinea, West Africa, using multipolarized ALOS PALSAR L-band data. *International Journal of Remote Sensing*, 34(2), 563–586. <https://doi.org/10.1080/01431161.2012.715773>.
- Flores-de-Santiago, F., Kovacs, J. M., & Flores-Verdugo, F. (2013b). The influence of seasonality in estimating mangrove leaf chlorophyll-a content from hyperspectral data. *Wetlands Ecology and Management*, 21(3), 193–207. <https://doi.org/10.1007/s11273-013-9290-x>.
- Flores-de-Santiago, F., Kovacs, J. M., Wang, J., Flores-Verdugo, F., Zhang, C., & González-Farías, F. (2016). Examining the influence of seasonality, condition, and species composition on mangrove leaf pigment contents and laboratory based spectroscopy data. *Remote Sensing*, 8(3), 226. <https://doi.org/10.3390/rs8030226>.
- Flores-Verdugo, F. J., Day, J. W., & Briseño-Dueñas, R. (1987). Structure, litter fall, decomposition, and detritus dynamics of mangroves in a Mexican coastal lagoon with an ephemeral inlet. *Marine Ecology Progress Series*, 35, 83–90. <https://doi.org/10.3354/meps035083>.
- Friess, D. A., & Webb, E. L. (2014). Variability in mangrove change estimates and implications for the assessment of ecosystem service provision. *Global Ecology and Biogeography*, 23(7), 715–725. <https://doi.org/10.1111/geb.12140>.
- Gao, J. (1998). A hybrid method toward accurate mapping of mangroves in a marginal habitat from SPOT multispectral data. *International Journal of Remote Sensing*, 19(10), 1887–1899. <https://doi.org/10.1080/014311698215045>.
- Giri, C., Ochieng, E., Tieszen, L. L., Zhu, Z., Singh, A., Loveland, T., Masek, J., & Duke, N. (2011). Status and distribution of mangrove forests of the world using earth observation satellite data. *Global Ecology and Biogeography*, 20(1), 154–159. <https://doi.org/10.1111/j.1466-8238.2010.00584.x>.
- Green, E. P., Clark, C. D., Mumby, P. J., Edwards, A. J., & Ellis, A. C. (1998). Remote sensing techniques for mangrove mapping. *International Journal of Remote Sensing*, 19(5), 935–956. <https://doi.org/10.1080/014311698215801>.
- Guo, M., Li, J., Sheng, C., Xu, J., & Wu, L. (2017). A review of wetland remote sensing. *Sensors*, 17(4), 777. <https://doi.org/10.3390/s17040777>.
- Heenkenda, M. K., Joyce, K. E., Maier, S. W., & Bartolo, R. (2014). Mangrove species identification: Comparing WorldView-2 with aerial photographs. *Remote Sensing*, 6(7), 6064–6088. <https://doi.org/10.3390/rs6076064>.
- Heenkenda, M. K., Joyce, K. E., Maier, S. W., & Bruin, S. D. (2015). Quantifying mangrove chlorophyll from high spatial resolution imagery. *ISPRS Journal of Photogrammetry and Remote Sensing*, 108, 234–244. <https://doi.org/10.1016/j.isprsjprs.2015.08.003>.
- Horstman, E. M., Dohmen-Janssen, C. M., Bouma, T. J., & Hulscher, S. J. M. H. (2015). Tidal-scale flow routing and sedimentation in mangrove forests: Combining field data and numerical modeling. *Geomorphology*, 228, 244–262. <https://doi.org/10.1016/j.geomorph.2014.08.011>.
- Ibharim, N. A., Mustapha, M. A., Lihan, T., & Mazlan, A. G. (2015). Mapping mangrove changes in the Matang mangrove forest using multi temporal satellite imageries. *Ocean and Coastal Management*, 114, 64–76. <https://doi.org/10.1016/j.ocecoaman.2015.06.005>.
- Jensen, R. J. (2016). *Introductory digital image processing: a remote sensing perspective*. Upper Saddle River: Prentice Hall 544 pp.
- Koedsin, W., & Vaiphasa, C. (2013). Discrimination of tropical mangroves at the species level with EO-1 Hyperion data. *Remote Sensing*, 5(7), 3562–3582. <https://doi.org/10.3390/rs5073562>.
- Kovacs, J. M. (2000). Perceptions of environmental change in a tropical coastal wetland. *Land Degradation and Development*, 11(3), 209–220. [https://doi.org/10.1002/1099-145X\(200005/06\)11:3<209::AID-LDR378>3.0.CO;2-Y](https://doi.org/10.1002/1099-145X(200005/06)11:3<209::AID-LDR378>3.0.CO;2-Y).
- Kovacs, J. M., Wang, J., & Blanco-Correa, M. (2001). Mapping disturbances in a mangrove forest using multi-date Landsat TM imagery. *Environmental Management*, 27(5), 763–776. <https://doi.org/10.1007/s002670010186>.
- Kovacs, J. M., Flores-Verdugo, F., Wang, J., & Aspden, L. P. (2004). Estimating leaf area index of a degraded mangrove forest using high spatial resolution satellite data. *Aquatic Botany*, 80(1), 13–22. <https://doi.org/10.1016/j.aquabot.2004.06.001>.
- Kovacs, J. M., Wang, J., & Flores-Verdugo, F. (2005). Mapping mangrove leaf area index at the species level using IKONOS and LAI-2000 sensors for the Agua Brava Lagoon, Mexican

- Pacific. *Estuarine, Coastal and Shelf Science*, 62(1-2), 377–384. <https://doi.org/10.1016/j.ecss.2004.09.027>.
- Kovacs, J. M., King, J. M. L., Flores-de-Santiago, F., & Flores-Verdugo, F. (2009). Evaluating the condition of a mangrove forest of the Mexican Pacific based on an estimated leaf area index mapping approach. *Environmental Monitoring and Assessment*, 157(1-4), 137–149. <https://doi.org/10.1007/s10661-008-0523-z>.
- Kovacs, J. M., Flores-de-Santiago, F., Bastien, J., & Lafrance, P. (2010). An assessment of mangroves in Guinea, West Africa, using a field and remote sensing based approach. *Wetlands*, 30(4), 773–782. <https://doi.org/10.1007/s13157-010-0065-3>.
- Kuenzer, C., Bluemel, A., Gebhardt, S., Quoc, T. V., & Dech, S. (2011). Remote sensing of mangrove ecosystems: a review. *Remote Sensing*, 3(12), 878–928. <https://doi.org/10.3390/rs3050878>.
- Lee, T. M., & Yeh, H. C. (2009). Applying remote sensing techniques to monitor shifting wetland vegetation: a case of study of Danshui river estuary mangrove communities, Taiwan. *Ecological Engineering*, 35(4), 487–496. <https://doi.org/10.1016/j.ecoleng.2008.01.007>.
- Li, X., Yeh, A. G. O., Wang, S., Liu, K., Liu, X., Qian, J., & Chen, X. (2007). Regression and analytical models for estimating mangrove wetland biomass in South China using Radarsat images. *International Journal of Remote Sensing*, 28(24), 5567–5582. <https://doi.org/10.1080/01431160701227638>.
- Lillesand, T. M., Kiefer, R. W., & Chapman, J. W. (2008). *Remote sensing and image interpretation*. New York: John Wiley & Sons.
- Martin, T. S. H., Olds, A. D., Pitt, K. A., Johnston, A. B., Butler, I. R., Maxwell, P. S., & Connolly, R. M. (2015). Effective protection of fish on inshore coral reefs depends on the scale of mangrove-reef connectivity. *Marine Ecology Progress Series*, 527, 157–165. <https://doi.org/10.3354/meps11295>.
- McCarthy, M. J., Merton, E. J., & Muller-Karger, F. E. (2015). Improved coastal wetland mapping using very-high 2-meter spatial resolution imagery. *International Journal of Applied Earth Observation and Geoinformation*, 40, 11–18. <https://doi.org/10.1016/j.jag.2015.03.011>.
- Mukherjee, N., Sutherland, W. J., Dicks, L., Hugé, J., Koedam, N., & Dahdouh-Guebas, F. (2014). Ecosystem service valuations of mangrove ecosystems to inform decision making and future valuation exercises. *PLoS One*, 9(9), e107706. <https://doi.org/10.1371/journal.pone.0107706>.
- Ose, K. (2015). Geosud Toa Reflectance. QGIS Python Plugins Repository. <https://plugins.qgis.org/plugins/geosudRefToa/>. Accessed 14 Nov 2017.
- Otero, V., Quisthoudt, K., Koedam, N., & Dahdouh-Guebas, F. (2016). Mangroves at their limits: Detection and area estimation of mangroves along the Sahara desert coast. *Remote Sensing*, 8(6), 512. <https://doi.org/10.3390/rs8060512>.
- Pettorelli, N. (2013). *The normalized differential vegetation index*. Oxford: Oxford University Press. <https://doi.org/10.1093/acprof:osobl/9780199693160.001.0001>.
- Pettorelli, N., Lurance, W. F., O'Brien, T. G., Wegmann, M., Nagendra, H., Turner, W., & Milner-Gulland, E. J. (2014). Satellite remote sensing for applied ecologists: opportunities and challenges. *Journal of Applied Ecology*, 51(4), 839–848. <https://doi.org/10.1111/1365-2664.12261>.
- Richter, R., & Schläpfer, D. (2016). Atmospheric / topographic correction for satellite imagery. ATCOR-2/3 User Guide, Version 9.0.2. http://www.rese.ch/pdf/atcor3_manual.pdf. Accessed 14 Nov 2017.
- Saintilan, N., Wilson, N. C., Rogers, K., Rajkaran, A., & Krauss, K. W. (2014). Mangrove expansion and salt marsh decline at mangrove poleward limits. *Global Change Biology*, 20(1), 147–157. <https://doi.org/10.1111/gcb.12341>.
- Son, N. T., Thanh, B. X., & Da, C. T. (2016). Monitoring mangrove forest changes from multi-temporal Landsat data in Can Gio biosphere reserve, Vietnam. *Wetlands*, 36(3), 565–576. <https://doi.org/10.1007/s13157-016-0767-2>.
- Troche-Souza, C., Rodriguez-Zuñiga, M. T., Velázquez-Salazar, S., Valderrama-Landeros, L., Villeda-Chávez, E., Alcántara-Maya, A., Vázquez-Balderas, B., Cruz-López, M. I., & Ressler, R. (2016). *Manglares de México: extensión, distribución y monitoreo (1970/1980–2015)*. Mexico City: CONABIO.
- Van Bochove, J. W., Sullivan, E., & Nakamura, T. (2014). *The importance of mangroves to people: A call to action*. Cambridge: United Nations Environment Programme World Conservation Monitoring Centre.
- Vo, T. Q., Kuenzer, C., & Oppelt, N. (2015). How remote sensing supports mangrove ecosystem service valuation: a case study in Ca Mau province, Vietnam. *Ecosystem Services*, 14, 67–75.
- Walters, B. B., Rönnbäck, P., Kovacs, J. M., Crona, B., Hussain, S. A., Badola, R., Primavera, J. H., Barbier, E., & Dahdouh-Guebas, F. (2008). Ethnobiology, socio-economics and management of mangrove forests: a review. *Aquatic Botany*, 89(2), 220–236. <https://doi.org/10.1016/j.aquabot.2008.02.009>.
- Wang, T., Zhang, H., Lin, H., & Fang, C. (2016). Textural-spectral feature-based species classification of mangroves in Mai Po Nature Reserve from Worldview-3 imagery. *Remote Sensing*, 8, 24.
- Ximenes, A. C., Maeda, E. E., Arcoverde, G. F. B., & Dahdouh-Guebas, F. (2016). Spatial assessment of the bioclimatic and environmental factors driving mangrove tree species' distribution along the Brazilian coastline. *Remote Sensing*, 8(6), 451. <https://doi.org/10.3390/rs8060451>.
- Zhang, C., Kovacs, J. M., Liu, Y., Flores-Verdugo, F., & Flores-de-Santiago, F. (2014). Separating mangrove species and conditions using laboratory hyperspectral data: A case study of a degraded mangrove forest of the Mexican Pacific. *Remote Sensing*, 6(12), 11673–11688. <https://doi.org/10.3390/rs61211673>.